Journal of Photochemistry and Photobiology A: Chemistry 221 (2011) 143–147

Contents lists available at ScienceDirect

Journal of Photochemistry and Photobiology A: Chemistry

journal homepage: www.elsevier.com/locate/jphotochem

Theoretical calculation of the photo-induced electron transfer rate between a gold atom and a gold cation solvated in CCl_4

Hanning Chen, Mark A. Ratner, George C. Schatz*

Argonne-Northwestern Solar Energy Research Center, Department of Chemistry, Northwestern University, 2145 Sheridan Road, Evanston, IL 60208, United States

ARTICLE INFO

Article history:
Available online 10 May 2011

Keywords:
Photo-induced electron transfer
Density functional theory
Marcus theory

ABSTRACT

A theoretical calculation was performed to evaluate the photo-induced electron transfer (PIET) rate between a gold atom and a gold ion solvated in carbon tetrachloride (CCl_4) in the framework of Marcus electron transfer (ET) theory, including both solvent reorganization effects and electronic wavefunction coupling between the ET diabatic states. A novel component of this work involves calculation of the electronic coupling strength using a recently developed constrained real-time time-dependent density-functional-theory (CRT-TDDFT) method. It is found that the PIET rate reaches its maximum value at the electronic resonance wavelength regardless of the inter-particle separation, suggesting a strong correlation between PIET and light absorption. In comparison with thermally activated electron transfer (TAET) at room temperature, light irradiation is demonstrated to be much more efficient than thermal fluctuations in promoting long-range ET, at least for the most common situations, when the light travelling substantially exceeds thermal energy. This work is the first step towards a quantum theory of plasmon enhanced electron transfer, and the theory can also be used to calculate electron transfer rates quite generally for condensed phase problems.

1. Introduction

Many chemical reactions can be associated with electron transfer [1], in which an electron moves from a donor chemical species to an acceptor chemical species either through thermal fluctuation [2] or under light irradiation [3]. The wide-ranging importance of electron transfer phenomena was highlighted by the Nobel Prize in chemistry awarded to Rudolph A. Marcus, who first realized that the electron transfer (ET) rate, k_{ET}, is governed by three important factors, namely the driving force ΔG_0, the reorganization energy λ_0, and the electronic coupling strength J_0, as shown below in the Marcus formula in the high temperature limit [4]:

$$k_{ET} = \frac{2\pi}{\hbar}|J_0|^2 \frac{1}{\sqrt{4\pi\lambda_0 k_b T}} e^{-(\Delta G_0+\lambda_0)^2/4\lambda_0 k_b T} \quad (1)$$

Assuming the Born–Oppenheimer approximation, a system's total wavefunction, $\Psi(R, r)$, can be decomposed into a vibrational part, $\varphi_N(R)$, and an electronic part, $\psi_e(r)$,

$$\Psi(R, r) = \varphi_N(R)\psi_e(r) \quad (2)$$

Therefore, in Eq. (1), the density-weighted Franck–Condon factor (DWFC) of $(1/\sqrt{4\pi\lambda_0 k_b T})e^{-(\Delta G_0+\lambda_0)^2/4\lambda_0 k_b T}$ reflects the vibrational wavefunction overlap, $\langle\varphi_N(A)|\varphi_N(D)\rangle$, between the donor ($D$) and the acceptor ($A$), whereas J_0 is related to the electronic Hamiltonian coupling:

$$J_0 = \langle\psi_e(A)|\hat{H}_0|\psi_e(D)\rangle \quad (3)$$

Following its original application to the so-called "outer sphere" ET, which is primarily driven by thermal fluctuations in the solvation medium [5], Marcus theory has been successfully expanded to describe the so-called "inner sphere" ET in which structural change in the redox centers and their coordinated solvents, such as in the Creutz–Taube ion with mixed valence, play a dominant role [6].

A widely used manner to probe ET mechanism is to connect a donor and an acceptor by a typically conjugated molecular bridge to comprise the so-called D-B-A system [7–9], which ET rate heavily depends on the donor–acceptor separation primarily because of sensitivity of the bridge-mediated electronic wavefunction overlap with distance [10–12]. From a theoretical perspective, there has been a long-standing issue of the accuracy of the calculated electronic coupling strength until the recent development of constrained density functional theory (C-DFT) [13]. By applying a systematically determined position-dependent Hartree potential to impose charge localization on the reacting centers, C-DFT achieves a rather reliable description of ET diabatic states that is critical for evaluating ΔG_0, λ_0 and J_0. Once all of the three key parameters are known, we are in a good position to evaluate the ET rate according to the Marcus formalism.

* Corresponding author. Tel.: +1 847 491 5657; fax: +1 847 491 7713.
E-mail address: schatz@chem.northwestern.edu (G.C. Schatz).

1010-6030/$ – see front matter © 2011 Elsevier B.V. All rights reserved.
doi:10.1016/j.jphotochem.2011.04.021

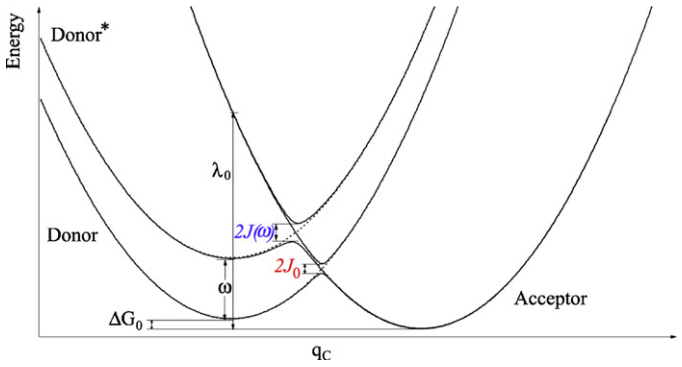

Fig. 1. Energy level diagram for a photo-induced electron transfer process as a function of the charge transfer coordinate q_C. For the present study, $\Delta G_0 = 0$.

In this paper we demonstrate the use of a new time-dependent density functional theory-based method, denoted CRT-TDDFT (constrained real-time TDDFT) [14], for performing this evaluation. Our goal with this approach is to develop a method which is suitable for modeling photoinduced ET processes involving plasmonic nanoparticles in which the photoexcitation is converted into electron transfer. Since plasmons are collective excitations of the conduction electrons, the process whereby their excitation leads to the transfer of individual electrons is not understood, yet there are experiments which clearly show that this can happen [15,16].

Plasmonic nanoparticles involve a large number of electrons, but they are also highly dissipative such that a time-domain theory can evaluate ET rates for a very large system using a short time integration. This is the principle of the CRT-TDDFT approach to calculating electron transfer rates [14]. The present application is designed to test this formalism for a very simple physical system which consists of a gold atom that transfers an electron to a gold ion in a non-aqueous solvent. Even for this very simple problem, we can study the dependence of the electron transfer rate on the frequency of the initial photoexcitation to see if electron transfer and optical absorption are correlated with each other. This is important for plasmonic processes where the quantum yield for photochemistry is not known, and where it is not clear that plasmon excitation couples to the electron being transferred. For individual gold atoms, the photoexcitation and electron transfer processes should be directly correlated if both atoms are well separated, but at shorter separations the donor and acceptor states are coupled, and more complex behavior is possible.

2. Computational details

Under light irradiation, the transferred electron is first promoted from the ground state donor to an excited state, followed by a non-radiative electronic coupling from the donor excited state to the acceptor to complete the PIET cycle (Fig. 1). The electronic coupling strength, $\langle \psi_D(t)|\hat{H}_0|\psi_A^0\rangle$, between the perturbed donor, $\psi_D(t)$, , and the unperturbed acceptor, ψ_A^0 is given by:

$$\begin{aligned}\langle \psi_D(t)|\hat{H}_0|\psi_A^0\rangle &= \langle \psi_D(t)|\psi_A^0\rangle \langle \psi_A^0|\hat{H}_0|\psi_A^0\rangle \\ &+ \langle \psi_D(t)|\psi_D^0\rangle \langle \psi_D^0|\hat{H}_0|\psi_A^0\rangle \\ &\approx \langle \psi_D(t)|\psi_A^0\rangle H_{AA}^0 + H_{AD}^0 \end{aligned} \quad (4)$$

under the assumption of a small perturbation that allows us to set

$$\langle \psi_D(t)|\psi_D^0\rangle \approx 1 \quad (5)$$

Here we note that we have assumed that there are only two states, Donor and Acceptor, and that these states are orthogonal and complete.

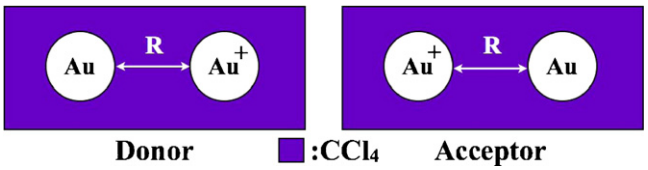

Fig. 2. Model system consisting of an ionized Au dimer solvated in CCl_4.

There are two ET paths indicated by Eq. (4). The first path is independent of the applied external field, involving the time-independent coupling strength H_{AD}^0 and coupling the ground states of the donor and acceptor, while the second path is via the excited states with a time-dependent coupling strength $\langle \psi_D(t)|\psi_A^0\rangle H_{AA}^0$ which is proportional to the applied field of the electromagnetic wave. The second term can be calculated by tracking the time evolution of the diabatic wavefunction overlap. In our recently formulated CRT-TDDFT [14], a C-DFT calculation is first performed to determine the constraining Hartree potentials for the construction of the diabatic ground states (i.e., for the donor and acceptor). These wavefunctions are then driven by an external electric field $E_{ext}(t)$ to mimic the effects of light irradiation, leading to a time dependent wavefunction $\psi_D(t)$. According to the definition of the frequency-dependent ET matrix element, $\gamma(\omega)$:

$$\gamma(\omega) = \frac{J(\omega)}{E_{ext}(\omega)} = \frac{\int dt e^{i\omega t} J(t)}{\int dt e^{i\omega t} E_{ext}(t)} = \frac{\int dt e^{i\omega t} \langle \psi_D(t)|\psi_A^0\rangle H_{AA}^0}{\int dt e^{i\omega t} E_{ext}(t)} \quad (6)$$

the "effective" coupling strength via the excited states, $J(\omega)$, is therefore given by:

$$J(\omega) = \gamma(\omega) E_{ext}(\omega) = \gamma(\omega)\sqrt{I(\omega)} \quad (7)$$

where I is the radiation intensity. Note that to incorporate the effect of damping in a plasmonic system, the frequency ω in Eq. (6) needs to be taken to be complex (i.e., $\omega \to \omega + i\Gamma$), with an imaginary component that describes the damping rate, similar to what we used earlier in calculating the spectra of plasmonic structures [17].

In general, ΔG_0 and λ_0 are respectively determined by energetic changes in the reactive system itself and by solvation effects. However, in our simple model system of an ionized Au dimer solvated in CCl_4 with fixed inter-particle separation R (Fig. 2), there is no structural change in the Au dimer after electron transfer so only solvent reorganization needs to be included in the ET transfer rate expression. In this sense, the driving force, $\Delta G_0(\omega)$ subject to an incident light energy $\hbar\omega$, can be expressed as:

$$\Delta G_0(\omega) = \Delta G_0 - \hbar\omega = -\hbar\omega \quad (8)$$

i.e., $\Delta G_0 = 0$. In the present study, λ_0 is estimated from the implicit solvation energy penalty by forcing the solute atom and ion to adopt the acceptor's charge distribution while the dielectric solvent medium is optimized for the donor's charge distribution:

$$\lambda_0 = E_{sol}(D, A) - E_{sol}(A, A) \quad (9)$$

where the first letter in parenthesis indicates the solvent's dielectric configuration, and the second one denotes the solute's charge distribution.

3. Results and discussion

3.1. Reorganization energy λ_0

The APBS package [18] was chosen to solve the Poisson–Boltzmann (PB) equation to determine the reorganization energy at room temperature (298.15 K). In the PB calculation, a dielectric constant of 2.24 and a molecular radius of 2.76 Å were used for the implicit solvent CCl_4, while a dielectric constant of

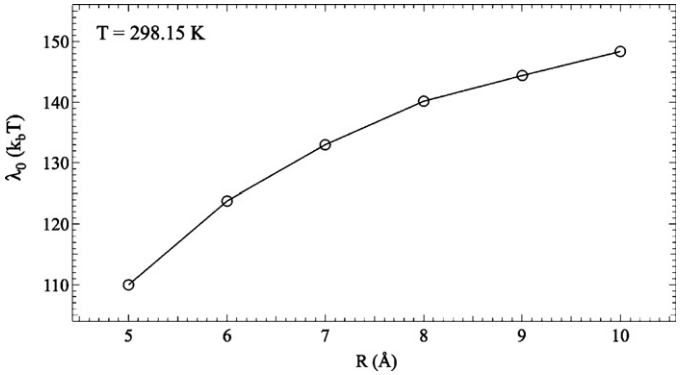

Fig. 3. Reorganization energy, λ_0, as a function of inter-particle separation, R.

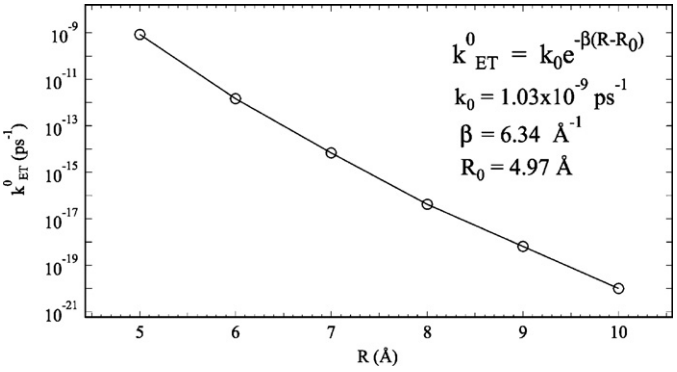

Fig. 5. Thermally activated electron transfer rate, k^0_{ET}.

1.0 and an atomic radius of 1.74 Å were selected for the solute Au atoms [19]. The electrostatic potentials at the atomic sites, $U_i(A)$ (i = 1, 2), were first evaluated with the acceptor's charge distribution (Q_1 = +1, Q_2 = 0) to obtain the solvation energy of the acceptor in the form:

$$E_{sol}(A, A) = \sum_i U_i(A)Q_i(A) \tag{10}$$

Moreover, with the electrostatic potentials, $U_i(A)$ (i = 1, 2), evaluated with the donor's charge distribution (Q_1 = 0, Q_2 = +1), acting on the acceptor's charge distribution,

$$E_{sol}(D, A) = \sum_i U_i(D)Q_i(A) \tag{11}$$

the reorganization energy λ_0 can be estimated as:

$$\lambda_0 = \sum_i (U_i(D) - U_i(A))Q_i(A) \tag{12}$$

We investigated λ_0 for a total of six inter-particle separations, R, varying from 5 Å to 10 Å, and the results indicate a strong position dependence (Fig. 3). When R is 5 Å, λ_0 reaches a small value of 110.0 k_bT (2.85 eV). With increasing R, λ_0 tends to approach a plateau value of >150.0 k_bT (3.88 eV). The larger reorganization energy corresponding to larger inter-particle separation can be ascribed to the better solvation of the isolated Au^+ cation.

3.2. Ground state electronic coupling strength J_0

The C-DFT method was employed to evaluate the ground state electronic coupling strength, J_0, between the donor and the acceptor diabatic states, using definitions that are illustrated in Fig. 2. It is not surprising that we see rapid decay of J_0 with increasing separation between the reaction centers in Fig. 4 due to the exponential radial character of the electronic wavefunctions. By fitting J_0 to a shifted exponential function,

$$J_0 = Je^{-\beta(R-R_0)} \tag{13}$$

the decay coefficient, β, turns out to be 1.43 Å^{-1}, which is substantially higher than with the bridged donor–acceptor system with β < 0.6 Å^{-1} [20–22]. The faster decay in our model Au dimer system arises from the wavefunction localization due to the missing π-stacking bridge.

3.3. Thermally activated electron transfer rate, k^0_{ET}

The thermally activated electron transfer rate, k^0_{ET}, (i.e., between the ground states of the donor and acceptor) is calculated according to Eq. (1), and is shown in Fig. 5. Although the k^0_{ET} is significantly lower than most experimentally reported values [4] (in the ps^{-1} range) due to the pronouncedly higher reorganization energy than what is commonly found, the exponential law is again perfectly satisfied with an even larger decay coefficient of 6.34 Å^{-1}. In this case, the variation of λ_0 with distance is not negligible, leading to a much stronger influence than the already rapid decay of J_0.

3.4. ET matrix element, $\gamma(\omega)$

The CP2K package [23] was used to perform C-DFT and the CRT-TDDFT calculations with the Perdew–Burke–Ernzerhof (PBE) [24] exchange-correlation functional and the polarized-valence-double-ζ (PVDZ) basis set [25]. A pulsed electric field was applied to the Au dimer with the polarization direction taken along the interatomic axis. An example of the time evolution of the electronic coupling strength driven by the external pulse is given in Fig. 6 for R = 5 Å. This exhibits very strong periodicity as expected. Through the Fourier transforms of $J(t)$ and $E_{ext}(t)$ according to Eq. (6), and

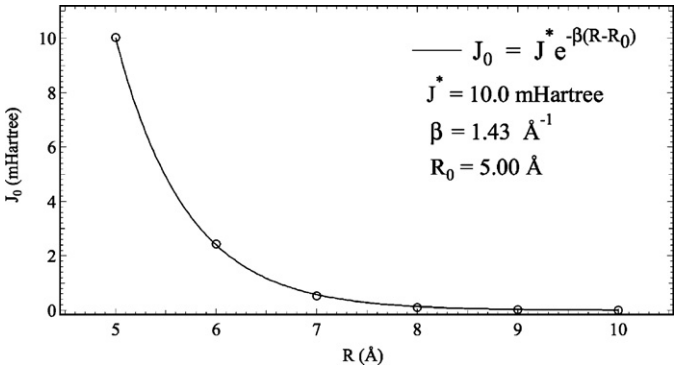

Fig. 4. The decay of electronic coupling strength, J_0 for ground state electron transfer.

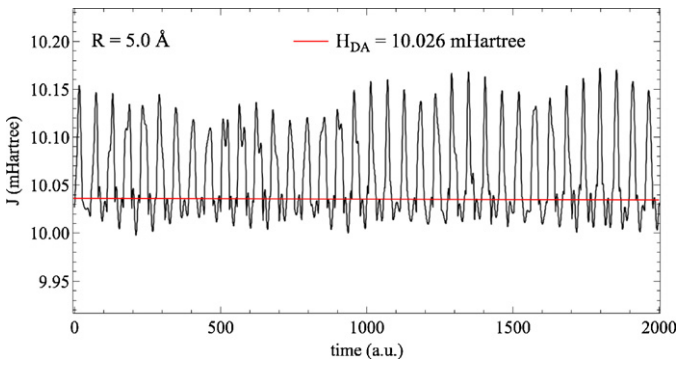

Fig. 6. Time evolution of electron coupling strength, $J(t)$, for R = 5.0 Å.

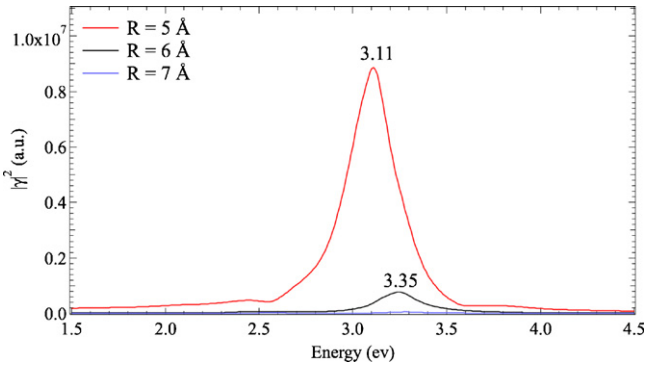

Fig. 7. The absolute square of the frequency-dependent ET matrix element, $|\gamma(\omega)|^2$.

using a damping constant $\Gamma = 0.1$ eV, the absolute square of the ET matrix element, $|\gamma(\omega)|^2$ for three inter-particle separations, 5 Å, 6 Å and 7 Å, are presented in Fig. 7. When $R = 5$ Å, $|\gamma(\omega)|^2$ has a pronounced peak at 3.11 eV with a height of $\sim 0.9 \times 10^7$ atomic unit (au). When R increases to 6 Å, a blue-shift of 0.24 eV is observed along with a drastically lowered peak height at $\sim 0.1 \times 10^7$ au. For the larger Au dimer separation of 7 Å, the peak of $|\gamma(\omega)|^2$ nearly disappears. A strong frequency dependence of $|\gamma(\omega)|^2$ is anticipated because the incident light wavelength not only determines the transition probability from the donor state to the excited state, but also determines the coupling efficiency between the excited state and the acceptor state. From a chemical kinetics perspective, the final production rate of the acceptor should be limited by either the transition probability or the coupling efficiency, whichever is slower. To exemplify the strong correlation between PIET and light absorption, the absorption cross-section, $\sigma(\omega)$, for the Au dimer with the same inter-particle separations is shown in Fig. 8. Apparently, $\sigma(\omega)$ follows a very similar pattern to $|\gamma(\omega)|^2$, i.e., a heightened peak at 3.05 eV for $R = 5$ Å, a blue-shift of ~0.16 eV when R increases to 6 Å, and comparable relative peak intensities. Note that the excitation energy associated with isolated gold atoms in CCl_4 is about 6 eV, so all the structures in Fig. 8 are associated with molecular excitation of the Au_2^+ dimer (Fig. 9).

3.5. Photo-induced electron transfer rate, $k_{ET}(\omega)$

The frequency-dependent PIET rate can be calculated by the revised Marcus formalism:

$$k_{ET}(\omega) = \frac{2\pi}{\hbar}\left|J(\omega)\right|^2 \frac{1}{\sqrt{4\pi\lambda_0 k_b T}} e^{-(\Delta G_0(\omega)+\lambda_0)^2/4\lambda_0 k_b T}$$
$$= \frac{2\pi}{\hbar} I(\omega)\left|\gamma(\omega)\right|^2 \frac{1}{\sqrt{4\pi\lambda_0 k_b T}} e^{-(-\hbar\omega+\lambda_0)^2/4\lambda_0 k_b T} \quad (14)$$

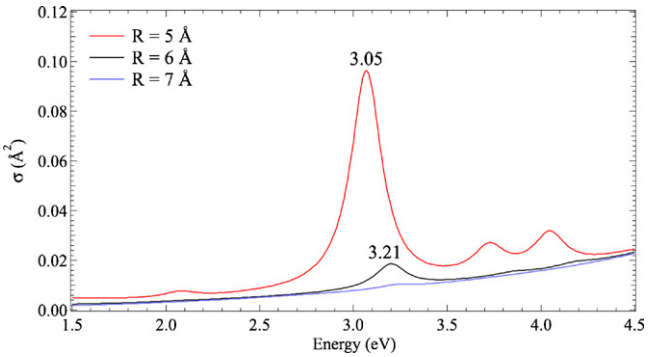

Fig. 8. Absorption cross-section of Au_2^+.

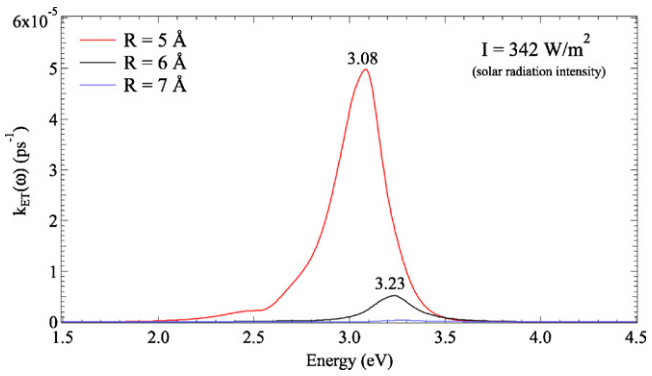

Fig. 9. Photo-induced electron transfer rate, $k_{ET}(\omega)$.

Obviously, the PIET rate, $k_{ET}(\omega)$, is governed by the radiation intensity, which determines the concentration of the transferring electrons in the excited state. In the present study, the average solar radiation intensity is taken to be 342 W/m^2 for all incident frequencies (a relatively weak intensity that is similar to values used in plasmon driven photochemistry experiments where nonlinear effects are unimportant). In addition, a short electric pulse with a field strength of 1.47×10^6 V/m was applied for 0.0121 fs to drive the electron dynamics. As anticipated, $k_{ET}(\omega)$ peaks at similar frequencies to $|\gamma(\omega)|^2$ and $\sigma(\omega)$, suggesting that the molecular resonance offers a unique opportunity to maximize the ET rate through quantum tunneling. By plotting $k_{ET}(\omega)$ at its resonance wavelength as a function of R (Fig. 10), and fitting it to a shifted exponential function as we did for k_{ET}^0, the decay coefficient, β, is found to be 2.27 Å^{-1}, much smaller than the 6.34 Å^{-1} value found for the decay of TAET. The much slower decay of PIET over this distance can be principally ascribed to the much more spatially extended molecular orbitals in excited states than in the ground state, leading to a much stronger electronic Hamiltonian coupling.

3.6. Comparison between $k_{ET}(\omega)$ and k_{ET}^0

To quantify the relative efficiency of PIET and TAET, an efficiency ratio, χ, is defined as:

$$\chi = \frac{k_{ET}(\omega_{res})}{k_{ET}^0} \quad (15)$$

where ω_{res} is the resonance frequency. For all inter-particle separations, PIET is substantially faster than TAET (Fig. 11). More interestingly, χ increases drastically from $\sim 6 \times 10^4$ at R=5 Å, to $\sim 1.7 \times 10^{10}$ at $R = 10$ Å. The high efficiency of PIET partially stems from the excellent match between the solvent reorganization energy, λ_0, and the molecular resonance energy, $\hbar\omega$, both being

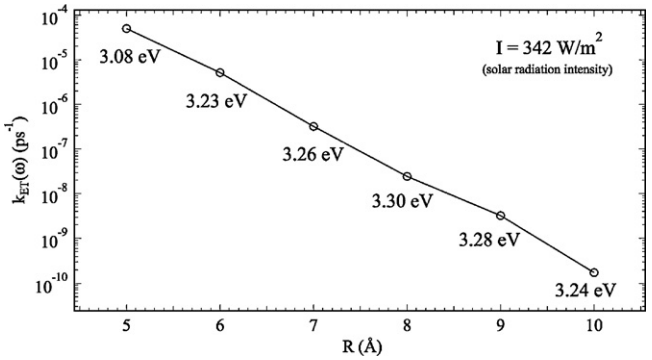

Fig. 10. Decay of photo-induced electron transfer rate, $k_{ET}(\omega)$ at its resonance energy (numbers under markers) with distance.

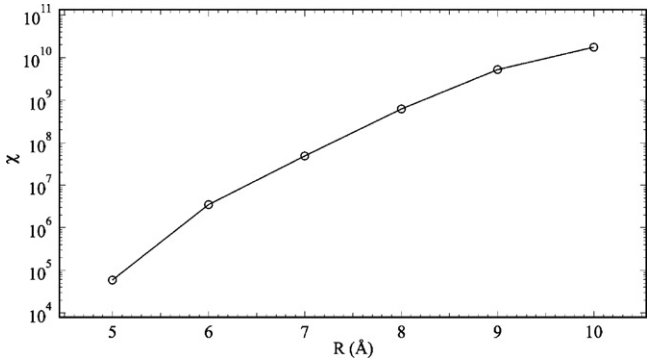

Fig. 11. Distance-dependent efficiency ratio, χ, between PIET and TAET.

~3.3 eV, leading to a maximum nuclear wavefunction overlap as quantified by the density weighted Franck–Condon factor. Another important contribution to the rapid ET under light irradiation is the more diffuse electronic wavefunctions associated with the excited states, making PIET more dominant over TAET as the separation of the two atoms increases.

4. Conclusions

For decades, the determination of the PIET rate has been a challenging task, as the calculation relies not only on the accurate construction of the diabatic ground states as needed for TAET without light irradiation, but also depends on the efficient evaluation of the electronic Hamiltonian coupling strength because a potentially large number of ET paths can be involved via different excited states. Inspired by time-dependent perturbation theory, our recently developed CRT-TDDFT approach [14] can efficiently determine the frequency-dependent electronic coupling strength between the excited state and the acceptor state by evaluating the transition probability from the donor state to the excited state, regardless of the degeneracy of the excited state. Because CRT-TDDFT is essentially a time-domain method, we avoid the explicit construction of the excited states, which is typically computationally expensive. As an added benefit, within a single CRT-TDDFT simulation run, the PIET rates for all incident wavelengths are determined through a Fourier transform of the time-dependent electronic coupling strength, in combination with a trivially devised driving field. Although the present application to Au-Au^+ is a "toy" problem and therefore is not computationally challenging, the CRT-TDDFT approach scales well with system size, and therefore should be applicable to many interesting photo-induced phenomena, including the plasmonic particle problems that have served as the primary guide in developing the Au dimer model. In addition we expect that additional applications will be possible, including electron injection from a light-harvesting dye to a semi-conductor layer in dye-sensitized solar cell [26], and water splitting under visible light irradiation on a catalytic surface [27].

Acknowledgments

The research was supported by the ANSER Energy Frontier Research Center (DE-SC0001785) and by grant DE-SC0004752 funded by the US Department of Energy, Office of Science, Office of Basic Energy Sciences. The computational resources utilized in this research were provided by Shanghai Supercomputer Center.

References

[1] R.A. Marcus, Chemical and electrochemical electron-transfer theory, Annu. Rev. Phys. Chem. 15 (1964) 155–196.
[2] S.S. Skourtis, D.H. Waldeck, D.N. Beratan, Fluctuations in biological and bioinspired electron-transfer reactions, Annu. Rev. Phys. Chem. 61 (2010) 461–485.
[3] P. Piotrowiak, Photoinduced electron transfer in molecular systems: recent developments, Chem. Soc. Rev. 28 (1999) 143–150.
[4] R.A. Marcus, N. Sutin, Electron transfers in chemistry and biology, Biochim. Biophys. Acta Bioenerg. 811 (1985) 265–322.
[5] R.A. Marcus, On the theory of oxidation–reduction reactions involving electron transfer I, J. Chem. Phys. 24 (1956) 966–978.
[6] D.E. Richardson, H. Taube, Mixed-valence molecules: electronic delocalization and stabilization, Coord. Chem. Rev. 60 (1984) 107–129.
[7] A.B. Ricks, G.C. Solomon, M.T. Colvin, A.M. Scott, K. Chen, M.A. Ratner, M.R. Wasielewski, Controlling electron transfer in donor, bridge, acceptor molecules using cross-conjugated bridges, J. Am. Chem. Soc. 132 (2010) 15427–15434.
[8] M.R. Hartings, I.V. Kurnikov, A.R. Dunn, J.R. Winkler, H.B. Gray, M.A. Ratner, Electron tunneling through sensitizer wires bound to proteins, Coord. Chem. Rev. 254 (2010) 248–253.
[9] R.H. Goldsmith, L.E. Sinks, R.F. Kelley, L.J. Betzen, W. Liu, E.A. Weiss, M.A. Ratner, M.R. Wasielewski, Wire-like charge transport at near constant bridge energy through fluorene oligomers, Proc. Natl. Acad. Sci. U.S.A. 102 (2005) 3540–3545.
[10] P.F. Barbara, T.J. Meyer, M.A. Ratner, Contemporary issues in electron transfer research, J. Phys. Chem. 100 (1996) 13148–13168.
[11] V. Mujica, A. Nitzan, Y. Mao, W. Davis, M. Kemp, A. Roitberg, M.A. Ratner, Electron Transfer in Molecules and Molecular Wires: Geometry Dependence, Coherent Transfer, and Control, John Wiley & Sons, Inc., 1999.
[12] O.S. Wenger, How donor, bridge, acceptor energetics influence electron tunneling dynamics and their distance dependences, Acc. Chem. Res. 44 (2010) 25–35.
[13] Q. Wu, T. Van Voorhis, Extracting electron transfer coupling elements from constrained density functional theory, J. Chem. Phys. 125 (2006) 164105–164109.
[14] H. Chen, M.A. Ratner, G.C. Schatz, Time-dependent theory of the rate of photoinduced electron transfer. J. Phys. Chem. B. in preparation.
[15] R. Jin, Y. Cao, C.A. Mirkin, K.L. Kelly, G.C. Schatz, J.G. Zheng, Photoinduced conversion of silver nanospheres to nanoprisms, Science 294 (2001) 1901–1903.
[16] R. Jin, Y.C. Cao, E. Hao, G.S. Metraux, G.C. Schatz, C.A. Mirkin, Controlling anisotropic nanoparticle growth through plasmon excitation, Nature 425 (2003) 487–490.
[17] H. Chen, M.A. Ratner, G.C. Schatz, Classical electrodynamics coupled to quantum mechanics for calculation of molecular optical properties: a RT-TDDFT/FDTD approach, J. Phys. Chem. C 114 (2010) 14384–14392.
[18] N.A. Baker, D. Sept, S. Joseph, M.J. Holst, J.A. McCammon, Electrostatics of nanosystems: application to microtubules and the ribosome, Proc. Natl. Acad. Sci. U.S.A. 98 (2001) 10037–10041.
[19] W.M. Haynes, CRC Handbook of Chemistry and Physics, 91 ed., CRC Press, New York, 2010.
[20] F.D. Lewis, T. Wu, Y. Zhang, R.L. Letsinger, S.R. Greenfield, M.R. Wasielewski, Distance-dependent electron transfer in DNA hairpins, Science 277 (1997) 673–676.
[21] M.R. Arkin, E.D.A. Stemp, R.E. Holmlin, J.K. Barton, A. Hörmann, E.J.C. Olson, P.F. Barbara, Rates of DNA-mediated electron transfer between metallointercalators, Science 273 (1996) 475–480.
[22] S. Priyadarshy, S.M. Risser, D.N. Beratan, DNA is not a molecular wire: protein-like electron-transfer predicted for an extended π-electron system, J. Phys. Chem. 100 (1996) 17678–17682.
[23] J. VandeVondele, M. Krack, F. Mohamed, M. Parrinello, T. Chassaing, J.R. Hutter, Quickstep: fast and accurate density functional calculations using a mixed Gaussian and plane waves approach, Comput. Phys. Commun. 167 (2005) 103–128.
[24] J.P. Perdew, K. Burke, M. Ernzerhof, Generalized gradient approximation made simple, Phys. Rev. Lett. 77 (1996) 3865.
[25] D.E. Woon, J.T.H. Dunning, Gaussian basis sets for use in correlated molecular calculations. IV. Calculation of static electrical response properties, J. Chem. Phys. 100 (1994) 2975–2988.
[26] S.D. Standridge, G.C. Schatz, J.T. Hupp, Distance dependence of plasmon-enhanced photocurrent in dye-sensitized solar cells, J. Am. Chem. Soc. 131 (2009) 8407–8409.
[27] A. Kudo, Y. Miseki, Heterogeneous photocatalyst materials for water splitting, Chem. Soc. Rev. 38 (2009) 253–278.